

05

## Local structure of amorphous $(\text{GeTe})_x(\text{Sb}_2\text{Te}_3)$ films

© A.V. Marchenko,<sup>1</sup> E.I. Terukov,<sup>2,3</sup> F.S. Nasredinov,<sup>4</sup> Yu.A. Petrushin,<sup>1</sup> P.P. Seregin<sup>1</sup>

<sup>1</sup> Herzen State Pedagogical University of Russia, St. Petersburg, Russia

<sup>2</sup> Ioffe Institute, St. Petersburg, Russia

<sup>3</sup> St. Petersburg State Electrotechnical University „LETI“, St. Petersburg, Russia; Ioffe Institute, St. Petersburg, Russia

<sup>4</sup> Peter the Great Saint-Petersburg Polytechnic University, St. Petersburg, Russia

e-mail: ppseregin@mail.ru

Received July 20, 2022

Revised July 20, 2022

Accepted August 8, 2022

By the method of Mossbauer spectroscopy on the isotope  $^{119}\text{Sn}$ , it was shown that tetravalent germanium atoms in amorphous films  $(\text{GeTe})_x(\text{Sb}_2\text{Te}_3)$  (where  $x = 0.5, 1, 2, 3$ ) form a tetrahedral system of chemical bonds, and in their local environment there are mainly tellurium atoms. In crystalline films  $(\text{GeTe})_x(\text{Sb}_2\text{Te}_3)$  is divalent hexacoordinated germanium at positions 4 *b* of the NaCl type crystal lattice. By the method of Mossbauer spectroscopy on  $^{121}\text{Sb}$  and  $^{125}\text{Te}$  atoms, it was shown that the amorphization of  $(\text{GeTe})_x(\text{Sb}_2\text{Te}_3)$  films does not change the local environment of antimony and tellurium atoms

**Keywords:** amorphous films, phase memory, Mossbauer spectroscopy.

DOI: 10.21883/TP.2022.11.55175.186-22

### Introduction

Chalcogenide alloys  $(\text{GeTe})_x(\text{Sb}_2\text{Te}_3)$  (where  $x = 0.5, 1, 2, 3$ ) are considered promising materials for data storage and coding in non-volatile memory devices [1]. The prerequisites for this are the significant contrast in conductivity and reflectivity between the crystalline and amorphous phases, as well as the reversibility and short transition time from crystalline to amorphous state [2]. Obviously, the requirements of miniaturization of memory devices and increasing the density of information recording in them are faced with the need to understand the details of the microstructure of the named materials in the crystalline and amorphous states.

The crystal structures of  $(\text{GeTe})_x(\text{Sb}_2\text{Te}_3)$  alloys have been studied in detail [3–8]. As for their amorphous modifications, many studies have been done to determine the near-order structure [9–15] in them, but a comparison of all the experimental data shows that these structures are still a matter of discussion [2,3,15]. In particular, apparent contradictions in the interpretation of experimental results obtained in the study of amorphous films  $\text{Ge}_2\text{Sb}_2\text{Te}_5$  by X-ray absorption fine structure spectroscopy (XAFS) [9–12]. This indicates the need to use additional experimental methods sensitive to minor changes in the local structure and in the population of the electron shells of atoms during the transition from amorphous to crystalline state.

Mossbauer spectroscopy (MS) is an effective tool for detecting changes in the local environment of atoms and their electronic structure during amorphization of  $\text{GeSbTe}$  alloys. In particular, this has been demonstrated in works [16,17], in which the MS method on impurity atoms  $^{119}\text{Sn}$  found that the amorphization of  $\text{GeAsTe}$  alloys (chemical analogues of

$(\text{GeTe})_x(\text{Sb}_2\text{Te}_3)$ ) is accompanied by changes in the near-order structure of germanium atoms.

A commonly cited disadvantage of MS is the limited number of probes (Mossbauer isotopes) that can be used for such studies. However, in  $\text{GeSbTe}$  alloys, all atoms have Mossbauer isotopes ( $^{73}\text{Ge}$ ,  $^{121}\text{Sb}$  and  $^{125}\text{Te}$ ) with satisfactory values of nuclear parameters, so that all atoms in  $\text{GeSbTe}$  type films can be the subject of Mossbauer studies without any restrictions. In particular, this was illustrated in [18] work on the study of the crystal–amorphous state transition in  $\text{Ge}_2\text{Sb}_2\text{Te}_5$  films by the MS method on  $^{121}\text{Sb}$  and  $^{125}\text{Te}$  probes. However, the authors of works [18,19] also demonstrated the possibility of studying compounds of the  $\text{Ge}_2\text{Sb}_2\text{Te}_5$  type using the MS method on impurity tin atoms. Both the absorption variant with the isotope  $^{119}\text{Sn}$  and the emission variant with the parent atoms  $^{119}\text{Sb}$  and  $^{119\text{m}}\text{Te}$ , when the a priori possibility of entering the Mossbauer probe  $^{119}\text{Sn}$  in any sites of crystalline and amorphous material is realized, were used.

However, apart from the work [18,19], as well as work [20], which shows the Mossbauer spectra  $^{121}\text{Sb}$  crystal compounds  $\text{GeSb}_2\text{Te}_4$ ,  $\text{Ge}_2\text{Sb}_2\text{Te}_5$  and  $\text{GeSb}_4\text{Te}_7$ , there are no Mossbauer studies of ternary  $(\text{GeTe})_x(\text{Sb}_2\text{Te}_3)$  compounds. In addition, we can mention the works [16,17,21–23], in which the structure of glassy binary alloys  $\text{Ge}_x\text{Te}_{1-x}$  was studied by the MS method on impurity atoms  $^{119}\text{Sn}$ . In particular, it has been shown that the coordination and valence states of the germanium atoms change during amorphization [16,17,22,23], and the local structure of germanium sites in amorphous  $\text{Ge}_x\text{Te}_{1-x}$  ( $x < 0.2$ ) [21] alloys has been described. The same  $\text{Ge}_x\text{Te}_{1-x}$  alloys in glassy and crystalline states were investigated by absorption MS on the isotope  $^{125}\text{Te}$  [24,25] and emission MS with parent atoms  $^{129}\text{Te}$  [25,26]. Finally, the authors [27] by

emission MS on the  $^{57}\text{Fe}$  isotope with parent nuclei  $^{57}\text{Mn}$  implanted in amorphous and crystalline GeTe films showed a difference in the near-order structures of these materials.

The present work is devoted to the study of the local structure of crystalline and amorphous films  $\text{Ge}_3\text{Sb}_2\text{Te}_6$ ,  $\text{Ge}_2\text{Sb}_2\text{Te}_5$ ,  $\text{GeSb}_2\text{Te}_4$  and  $\text{GeSb}_4\text{Te}_7$  by absorption MS on isotopes  $^{119}\text{Sn}$ ,  $^{121}\text{Sb}$  and  $^{125}\text{Te}$ .

## 1. Experimental procedure

X-ray amorphous films  $a\text{-Ge}_3\text{Sb}_2\text{Te}_6$ ,  $a\text{-Ge}_2\text{Sb}_2\text{Te}_5$ ,  $a\text{-GeSb}_2\text{Te}_4$ ,  $a\text{-GeSb}_4\text{Te}_7$  (denote them  $a\text{-GeSbTe}$ ),  $a\text{-Ge}_{1.5}\text{Te}_{8.5}$  and tin-doped X-ray amorphous films  $a\text{-Ge}_{2.95}\text{Sn}_{0.05}\text{Sb}_2\text{Te}_6$ ,  $a\text{-Ge}_{1.95}\text{Sn}_{0.05}\text{Sb}_2\text{Te}_5$ ,  $a\text{-Ge}_{0.95}\text{Sn}_{0.05}\text{Sb}_2\text{Te}_4$  and  $a\text{-Ge}_{0.95}\text{Sn}_{0.05}\text{Sb}_4\text{Te}_7$  (denote them  $a\text{-Ge}(\text{Sn})\text{SbTe}$ ) and  $a\text{-Ge}_{1.45}\text{Sn}_{0.05}\text{Te}_{8.5}$  of thickness  $3\mu\text{m}$  were obtained by magnetron sputtering of polycrystalline targets of similar composition at constant current in a nitrogen atmosphere on aluminum foil substrates. Then, the films were annealed in the temperature range  $150\text{--}200^\circ\text{C}$  to obtain crystalline films. The isotope used for the syntheses was  $^{119}\text{Sn}$  of 96% enrichment. The film composition was monitored by X-ray fluorescence analysis.

Ge(Sn) tin-doped germanium samples were obtained by fusing metallic tin and germanium. For this purpose, a single-crystal plate of chemically etched germanium (unalloyed, with an electron concentration of less than  $10^{14}\text{cm}^{-3}$ ) of  $200\mu\text{m}$  thickness was used. A film of metallic tin (enriched up to 96% with the isotope  $^{119}\text{Sn}$ ) was sputtered on the plate. The melting was carried out in an evacuated quartz ampoule at  $800^\circ\text{C}$ , then the ampoule was slowly cooled to  $400^\circ\text{C}$  and then quenched in air. After annealing, the sample was washed with a hot mixture of  $\text{HCl}+\text{HF}$  to remove tin residues from the surface. According to work [28], the solubility of tin in germanium under these conditions is about 1 at.%, which provides a surface absorber density of  $\sim 0.1\text{mg}/\text{cm}^2$  by  $^{119}\text{Sn}$ .

Mossbauer spectra were taken on a CM 4201 TerLab spectrometer at 80 K. The spectra of  $^{119}\text{Sn}$ ,  $^{121}\text{Sb}$ , and  $^{125}\text{Te}$  were measured using  $\text{Ca}^{119\text{mm}}\text{SnO}_3$ ,  $\text{Ca}^{121}\text{SnO}_3$  and  $\text{Mg}_3^{125\text{m}}\text{TeO}_6$ , respectively. Isomeric shifts  $\delta$  spectra of  $^{119}\text{Sn}$ ,  $^{121}\text{Sb}$  and  $^{125}\text{Te}$  are given relative to the  $\text{CaSnO}_3$ ,  $\text{InSb}$  and  $\text{Mg}_3\text{Te}_6$  absorbers, respectively. The instrumental spectral line widths for the isotopes  $^{119}\text{Sn}$ ,  $^{121}\text{Sb}$  and  $^{125}\text{Te}$  were 0.79(2), 2.35(6) and 6.00(8) mm/s, respectively.

## 2. Experimental results

The Mossbauer spectra of impurity atoms  $^{119}\text{Sn}$  in amorphous and crystalline films of  $\text{Ge}(\text{Sn})\text{SbTe}$  and  $\text{Ge}_{1.45}\text{Sn}_{0.05}\text{Te}_{8.5}$  are shown in Fig. 1 and 2. All spectra are single lines with widths at half-height  $G \sim 1.30\text{--}1.36\text{mm/s}$  (for the spectrum of  $c\text{-Ge}_{1.45}\text{Sn}_{0.05}\text{Te}_{8.5}$  film,  $G = 0.85\text{mm/s}$  was obtained). The spectra of amorphous films have isomeric shifts  $\delta \sim 2.03\text{--}2.09\text{mm/s}$ , for crystalline films  $\delta \sim 3.49\text{--}3.54\text{mm/s}$  was obtained.

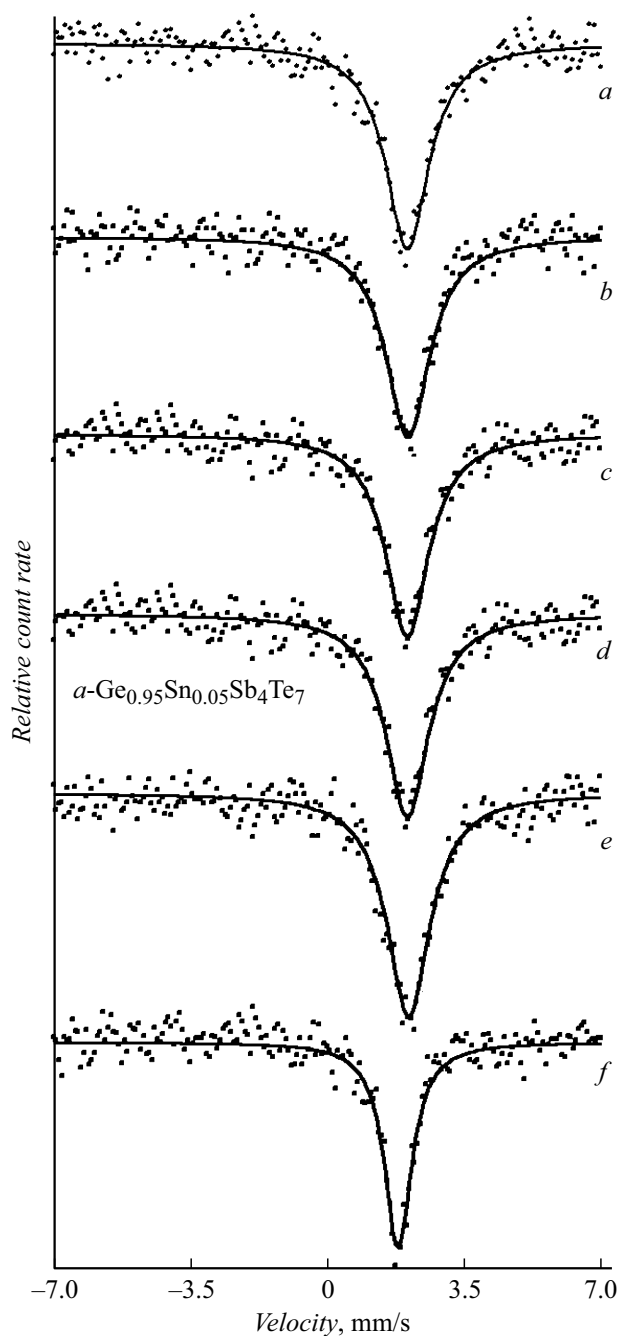


**Figure 1.** Mossbauer spectra of  $^{119}\text{Sn}$  films  $a\text{-Ge}_{2.95}\text{Sn}_{0.05}\text{Sb}_2\text{Te}_6$  (a),  $a\text{-Ge}_{1.95}\text{Sn}_{0.05}\text{Sb}_2\text{Te}_5$  (b),  $a\text{-Ge}_{0.95}\text{Sn}_{0.05}\text{Sb}_2\text{Te}_4$  (c),  $a\text{-Ge}_{0.95}\text{Sn}_{0.05}\text{Sb}_4\text{Te}_7$  (d),  $a\text{-Ge}_{1.45}\text{Sn}_{0.05}\text{Te}_{8.5}$  (e) and crystalline germanium (f) at 80 K.

The spectra of  $^{121}\text{Sb}$  films  $a\text{-GeSbTe}$  (Fig. 3) and films  $c\text{-GeSbTe}$  films (Fig. 4), as well as the spectrum of the compound  $\text{b}_2\text{Te}_3$  (Fig. 4) are single broadened lines ( $G \sim 5.4\text{--}5.7\text{mm/s}$ ), the isomeric shifts of which are in the range  $\delta \sim 5.1\text{--}5.5\text{mm/s}$ .

The spectra of  $^{125}\text{Te}$  films  $a\text{-GeSbTe}$  (Fig. 5),  $c\text{-GeSbTe}$  (Fig. 6), and  $\text{GeTe}$  and  $\text{Sb}_2\text{Te}_3$  compounds (Fig. 7) are single broadened lines ( $G \sim 6.90\text{mm/s}$ ) with iso-

meric shifts  $\delta \sim 1.32-1.39$  mm/s. The  $^{125}\text{Te}$  spectrum of the amorphous film  $a\text{-Ge}_{1.5}\text{Te}_8$  is a quadrupolar doublet (isomeric shift  $\delta = 1.65(4)$  mm/s, quadrupolar splitting  $QS = 8.41(8)$  mm/s). Crystallization of  $\text{Ge}_{1.5}\text{Te}_{8.5}$  films results in a two-phase mixture of tellurium (spectrum parameters:  $\delta = 1.73$  mm/s,  $QS = 7.10$  mm/s) and germanium telluride (spectrum parameters:  $\delta = 1.23$  mm/s,  $G = 6.90$  mm/s).

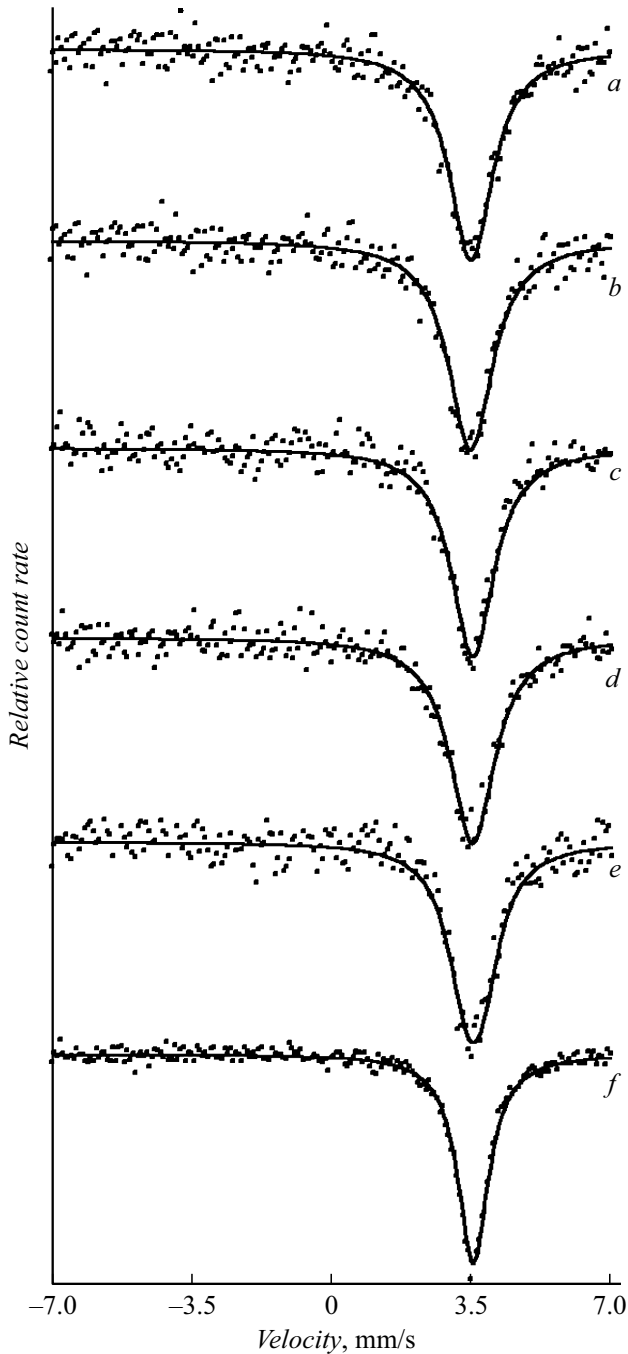


**Figure 2.** Messbauer spectra of  $^{119}\text{Sn}$  films  $c\text{-Ge}_{2.95}\text{Sn}_{0.05}\text{Sb}_2\text{Te}_6$  (a),  $c\text{-Ge}_{1.95}\text{Sn}_{0.05}\text{Sb}_2\text{Te}_5$  (b),  $c\text{-Ge}_{0.95}\text{Sn}_{0.05}\text{Sb}_2\text{Te}_4$  (c),  $a\text{-Ge}_{0.95}\text{Sn}_{0.05}\text{Sb}_4\text{Te}_7$  (d),  $c\text{-Ge}_{1.45}\text{Sn}_{0.05}\text{Te}_{8.5}$  (e) and compounds  $\text{SnTe}$  (f).

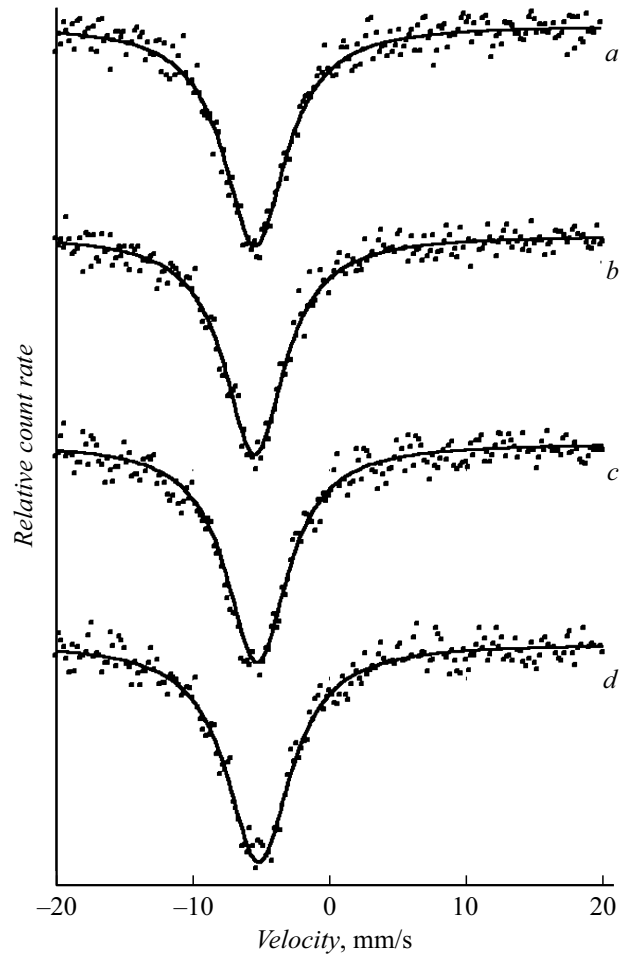


**Figure 3.** Messbauer spectra of  $^{121}\text{Sb}$  films  $a\text{-Ge}_3\text{Sb}_2\text{Te}_6$  (a),  $a\text{-Ge}_2\text{Sb}_2\text{Te}_5$  (b),  $a\text{-GeSb}_2\text{Te}_4$  (c) and  $a\text{-GeSb}_4\text{Te}_7$  (d).

### 3. Discussion of experimental results

#### 3.1. Germanium atoms in amorphous films

Germanium and tin are in the main subgroup IV of group D.I. Mendeleev table and when interpreting the parameters of the Messbauer spectra of impurity atoms  $^{119}\text{Sn}$  in crystalline and amorphous films  $\text{GeSb(Sn)Te}$  and  $\text{Ge}_{1.45}\text{Sn}_{0.05}\text{Te}_{8.5}$ , isovalent substitution of germanium for tin in the film structure was assumed.

Isomeric shifts of the spectra of impurity atoms  $^{119}\text{Sn}$  films  $a\text{-Ge(Sn)SbTe}$  and  $a\text{-Ge}_{1.45}\text{Sn}_{0.05}\text{Te}_{8.5}$  have values lying in the interval between the values of isomeric shifts of the spectrum of impurity atoms  $^{119}\text{Sn}$  in crystalline germanium ( $\delta = 1.80(1)$  mm/s, (Fig. 1)) and spectrum of gray tin  $\alpha\text{-Sn}$  ( $\delta = 2.10(1)$  mm/s). The isomeric shifts of the last two spectra form the region of isomeric shifts of tetravalent tin compounds with a tetrahedral  $sp^3$ -system of chemical bonds. In other words, the impurity tin atoms in the structure of  $a\text{-Ge(Sn)SbTe}$  and  $a\text{-Ge}_{1.45}\text{Sn}_{0.05}\text{Te}_{8.5}$  films isovalently replace the fourvalent germanium atoms, which form a tetrahedral chemical bond with atoms in their local

surroundings (i.e., the coordination number of germanium atoms is four).

In order to determine the chemical nature of the atoms in the vicinity of germanium atoms in  $a$ -GeSbTe films, we compared the isomeric shift values of the spectra of impurity tin atoms  $\delta$  in  $a$ -Ge(Sn)SbTe films ( $\delta \sim 2.03$ – $2.07$  mm/s) with values  $\delta$  in films  $a$ -Ge<sub>1.45</sub>Sn<sub>0.05</sub>Te<sub>8.5</sub> ( $\delta \sim 2.09$  mm/s, the local surroundings of germanium contain mainly tellurium atoms) and in crystalline germanium Ge(Sn) ( $\delta \sim 1.80$  mm/s, their local environment contains only germanium atoms). Based on the above data, we can conclude that the local environment of germanium in  $a$ -GeSbTe films contains predominantly tellurium atoms. This can be confirmed by the fact that the isomeric shift of the spectra <sup>119</sup>Sb films  $a$ -Ge(Sn)SbTe monotonically increases from the value 2.03(1) mm/s for the composition Ge<sub>3</sub>Sb<sub>2</sub>Te<sub>6</sub>

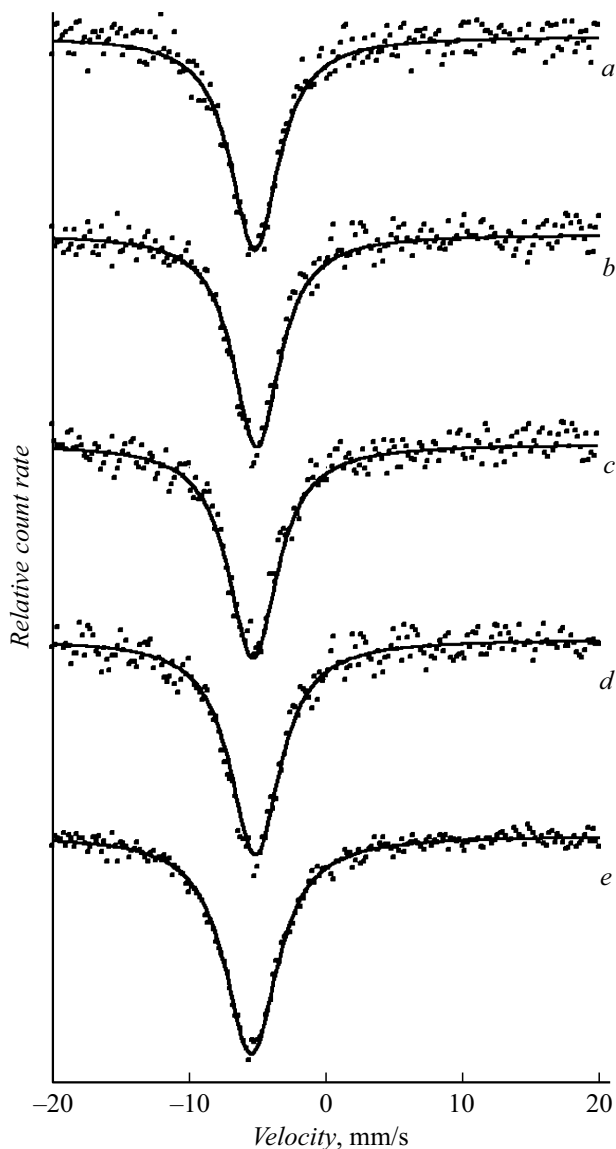


**Figure 4.** Messbauer spectra of <sup>121</sup>Sb films  $c$ -Ge<sub>3</sub>Sb<sub>2</sub>Te<sub>6</sub> (a),  $c$ -Ge<sub>2</sub>Sb<sub>2</sub>Te<sub>5</sub> (b),  $c$ -GeSb<sub>2</sub>Te<sub>4</sub> (c),  $a$ -GeSb<sub>4</sub>Te<sub>7</sub> (d) and the crystal compound Sb<sub>2</sub>Te<sub>3</sub> (e).

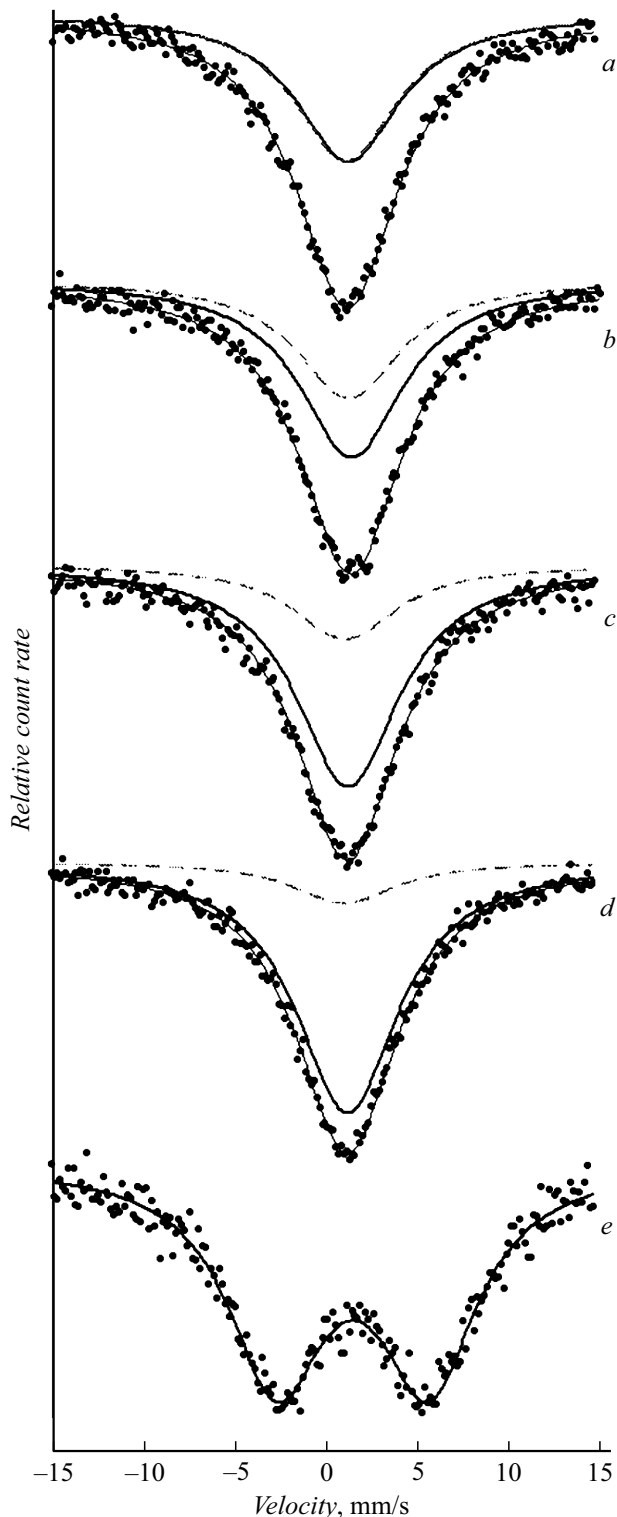


**Figure 5.** Messbauer spectra of <sup>125</sup>Te films  $a$ -Ge<sub>3</sub>Sb<sub>2</sub>Te<sub>6</sub> (a),  $a$ -Ge<sub>2</sub>Sb<sub>2</sub>Te<sub>5</sub> (b),  $a$ -GeSb<sub>2</sub>Te<sub>4</sub> (c),  $a$ -GeSb<sub>4</sub>Te<sub>7</sub> (d) and  $a$ -Ge<sub>1.5</sub>Te<sub>8.5</sub> (e). The experimental spectra of  $a$ -GeSbTe are shown to decompose into two singlet spectra corresponding to tellurium atoms, whose local surroundings are predominantly either germanium atoms (dashed line) or antimony atoms (solid line).

(containing 27.3 at.% Ge) to the value 2.07(1) mm/s for the composition  $\text{GeSb}_4\text{Te}_7$  (containing 8.3 at.% Ge).

Kolobov et al. [9], based on XAFS results, proposed the „mechanism of umbrella reversal“ to describe the order–free

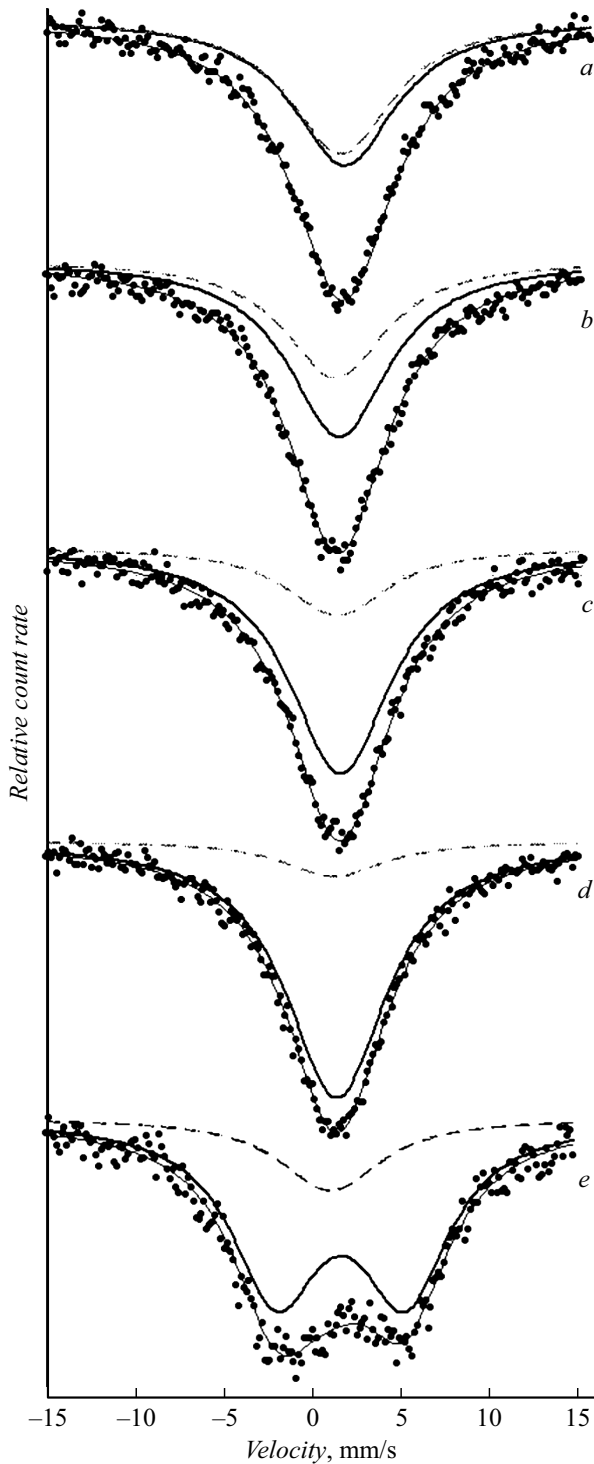


**Figure 6.** Messbauer spectra of  $^{125}\text{Te}$  films  $c\text{-Ge}_3\text{Sb}_2\text{Te}_6$  (a),  $c\text{-Ge}_2\text{Sb}_2\text{Te}_5$  (b),  $c\text{-GeSb}_2\text{Te}_4$  (c),  $c\text{-GeSb}_4\text{Te}_7$  (d) and  $c\text{-Ge}_{1.5}\text{Te}_{8.5}$  (e). The decomposition of the  $c\text{-Ge}_{1.5}\text{Te}_{8.5}$  experimental spectrum into a singlet and a quadrupolar doublet, corresponding to the GeTe and Te phases, respectively, is shown.

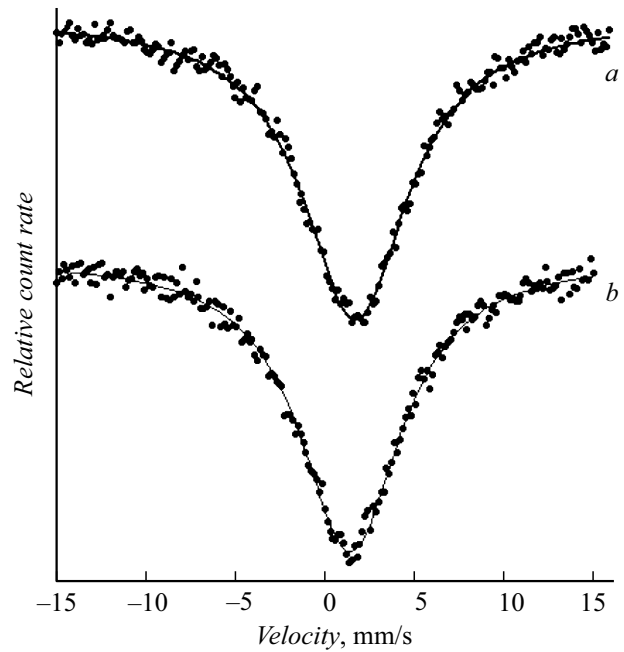


**Figure 7.** Messbauer spectra of  $^{125}\text{Te}$  compounds  $\text{GeTe}$  (a) and  $\text{Sb}_2\text{Te}_3$  (b).

order transition in  $\text{Ge}_2\text{Sb}_2\text{Te}_5$  films, according to which the amorphization of the crystal film is accompanied by a jump of the Ge atom from the octahedral position to the tetrahedral position surrounded by four Te atoms, and Ge–Ge bonds were not detected.

However, Baker et al. [10,11], also using EXAFS data for  $a\text{-Ge}_2\text{Sb}_2\text{Te}_5$ , concluded that Ge atoms participate in structural units of  $\text{Te}_3\text{Ge}\text{--}\text{GeTe}_3$ , and in contrast to the mechanism of umbrella flip this model is based on preferential Ge–Ge bond formation.

Also by EXAFS (combined with high-energy X-ray diffraction and neutron diffraction) the structure of amorphous compounds  $a\text{-Ge}_2\text{Sb}_2\text{Te}_5$  and  $a\text{-GeSb}_2\text{Te}_4$  was studied by the authors [12]. It was shown that Ge–Ge and Ge–Sb bonds are present in both amorphous compounds. All atoms satisfy formal valence requirements, with Ge having tetrahedral system of chemical bonds.

Finally, the local structure of the amorphous phase  $\text{Ge}_2\text{Sb}_2\text{Te}_5$  was investigated using anomalous X-ray scattering near the  $K$  absorption edges of germanium, antimony and tellurium atoms, and the data were analyzed using inverse Monte Carlo simulations [15]. It was found, that about half of the Ge atoms have an octahedral environment similar to that in the crystal. The remaining half of the Ge atoms with tetrahedral symmetry acts as its own energy barrier between the phases, providing a long lifetime of the amorphous  $\text{Ge}_2\text{Sb}_2\text{Te}_5$  modification.

Our MS data allow us to conclude that tetravalent germanium atoms form a tetrahedral  $sp^3$  system of chemical bonds in the structural grid of the amorphous matrix (local

coordination number of germanium atoms is four) and have mainly tellurium atoms in their closest environment.

Our MS data are in agreement with the authors' ideas [9] about the local structure of germanium atoms in the amorphous compounds  $\text{Ge}_2\text{Sb}_2\text{Te}_5$  and allow us to extend these ideas to other amorphous compounds  $a\text{-GeSbTe}$ : The tetravalent germanium atoms form a tetrahedral  $sp^3$ -system of chemical bonds in the structural grid of the amorphous matrix (the local coordination number is four) and have only tellurium atoms in their closest environment. It also confirms the conclusion of the authors [12] that in the amorphous compounds  $\text{Ge}_2\text{Sb}_2\text{Te}_5$  and  $\text{GeSb}_2\text{Te}_4$  the germanium atoms have a fourfold coordination (with the only specification that this is true for all the amorphous films  $a\text{-GaSbTe}$ ).

A characteristic feature of the spectra of impurity atoms  $^{119}\text{Sn}$  in  $a\text{-GeSbTe}$  films is their broadening. There could be two reasons for the widening.

First, possible distortions of the angles between the bonds of tin atoms with the atoms in its immediate vicinity should lead to a broadening of the spectrum due to unresolved quadrupolar splitting. Processing the experimental spectra under this assumption leads to quadrupolar splitting values of  $QS \leq 0.55$  mm/s. This  $QS$  value indicates a significant distortion of the tetrahedral valence angles.

The second reason for the broadening of the spectra — fluctuations in the bond lengths of Ge—Te while maintaining the tetrahedral bond angles. This will lead to spectrum broadening due to heterogeneous isomeric shift. In the first approximation, we can assume that the distribution of isomeric shift values obeys Gaussian law:

$$W = \frac{1}{\sigma\sqrt{2\pi}} \exp\left[-\frac{(\delta - \delta_0)^2}{2\delta^2}\right],$$

where  $\delta_0$  — the mean value of the isomeric shift,  $\delta$  — its standard deviation.

We performed a numerical calculation of the spectrum shape, and to agree its results with the experimental values of the spectra widths of amorphous films  $a\text{-Ge(Sn)SbTe}$ , it is necessary to take  $\sigma = (0.17\text{--}0.20)$  mm/s.

All observed isomeric shifts of the spectra  $^{119}\text{Sn}$  in the films  $a\text{-Ge(Sn)SbTe}$  and  $a\text{-Ge}_{1.45}\text{Sn}_{0.05}\text{Te}_{8.5}$ , determined by the position of their spectra centers of gravity, are less than the isomeric shift of the spectrum  $\alpha\text{-Sn}$ . This corresponds to the fact that the  $5s p^3$ -orbitals of tin are less than unity, the tin atoms have small positive effective charges, and the Sn—Te (and probably Ge—Te) bond is partially ionic. However, if we assume the above-mentioned distribution of isomeric shift values with a standard deviation of  $\sigma \sim 0.2$  mm/s, then about half of the shifts will be in the region of values with populations of  $5s p^3$ -orbitals greater than unity. Such settlements correspond to negative tin charges, which is hardly possible for the Sn—Te bond. The latter means that the broadening of the Messbauer spectral lines of  $^{119}\text{Sn}$  films  $a\text{-Ge(Sn)SbTe}$  cannot be explained by fluctuations in the Sn—Te bond lengths alone, and

distortions of the valence angles, which seem to be the main contributors to the broadening, must be considered.

### 3.2. Germanium atoms in $c\text{-GeSbTe}$ crystalline films

The impurity atom spectra of  $^{119}\text{Sn}$  of films  $c\text{-GeSbTe}$  and  $c\text{-Ge}_{1.45}\text{Sn}_{0.05}\text{Te}_{8.5}$  have isomeric shifts typical of the spectra of  $^{119}\text{Sn}$  ion compounds of divalent tin. For comparison, Fig. 2 shows the spectrum of the divalent tin compound  $\text{SnTe}$ , for which  $\delta = 3.54(1)$  mm/s.

According to [3–5],  $c\text{-GeSbTe}$  alloys can be obtained as metastable vacancy-unordered cubic phases by heating the amorphous film above the  $150^\circ\text{C}$  crystallization temperature. These phases have rhombohedral distorted NaCl-type lattices ( $Fm3m$ ) with stoichiometric vacancies. The anion-like positions are occupied by Te atoms, and the cation-like positions — by Ge, Sb atoms, and 20% of them are vacant. The XAFS [9] method demonstrated that the six neighboring Ge—Te bonds with octahedral symmetry sites are separated into three short and three long bonds, as in the GeTe-cristal [29].

The MS data on impurity atoms  $^{119}\text{Sn}$  for  $c\text{-Ge(Sn)SbTe}$  films are consistent with the results of X-ray diffraction studies of metastable vacancy-unordered cubic  $c\text{-GeSbTe}$  compounds. The divalent tin  $\text{Sn}^{2+}$  (electronic configuration  $5s^2 p^x$ ) replaces the divalent germanium  $\text{Ge}^{2+}$  (electronic configuration  $4s^2 p^x$ ) in the positions  $4b$  of the rhombohedral distorted lattice like NaCl, and only the tellurium atoms are in the immediate neighborhood of the six coordinated germanium atoms. The latter circumstance explains the proximity of the isomeric shifts of the spectra of the  $^{119}\text{Sn}$  compounds  $c\text{-GeSbTe}$  to the isomeric shift of the spectrum  $^{119}\text{Sn}$  compound  $\text{SnTe}$ , which also has a NaCl type lattice. The broadening of the spectra of ternary compounds in comparison with the width of the  $\text{SnTe}$  spectrum ( $G = 0.94$  mm/s) is associated with the rhombohedral distortion of the NaCl-type lattice of these compounds, as well as with a large concentration of randomly distributed stoichiometric vacancies.

Note that the change in the local structure of germanium atoms during amorphization of  $\text{GeSbTe}$  compounds (transition from the divalent six-coordinated state to the tetravalent four-coordinated state) is not unique to  $\text{GeSbTe}$  compounds, since a similar effect was observed earlier for alloys of the Ge—As—Te [16,17] system.

For the  $c\text{-Ge}_{1.45}\text{Sn}_{0.05}\text{Te}_{8.5}$  film, X-ray phase analysis showed the presence of two phases — the GeTe compound and elementary tellurium. The isomeric shift of the Messbauer spectrum  $^{119}\text{Sn}$  of this sample ( $\delta = 3.53(1)$  mm/s) is close in isomeric shift to that of the  $\text{SnTe}$  compound, but reveals a slightly larger width ( $G = 1.13(2)$  mm/s). In the system  $\text{Ge}_{1-x}\text{Sn}_x\text{Te}$ , there is a continuous series of solid solutions and, obviously, when the glass crystallizes, a solid solution of  $\text{Ge}_{1.45}\text{Sn}_{0.05}\text{Te}_{1.5}$  forms, which at 80 K has a rhombohedrically distorted NaCl [30] lattice structure. Breaking the cubic symmetry of the local environment of

the tin atoms in  $\text{Ge}_{1.45}\text{Sn}_{0.05}\text{Te}_{1.5}$  leads to an electric field gradient on the nuclei  $^{119}\text{Sn}$  and quadrupolar splitting of the spectrum. Therefore, we interpreted the broadening of the spectrum of  $c\text{-Ge}_{1.45}\text{Sn}_{0.05}\text{Te}_{1.5}$  films as a consequence of unresolved quadrupolar splitting. The obtained value of quadrupolar splitting ( $QS = 0.42(3)$  mm/c) indicates insignificant distortion of the octahedral environment of tin atoms, and we can assume that the coordination number of tin in the crystal sample is six.

### 3.3. An antimony atoms in amorphous and crystalline GeSbTe films

The isomeric shifts of the  $^{121}\text{Sb}$  spectra of the  $a\text{-GeSbTe}$  and  $c\text{-GeSbTe}$  films, as well as the spectra of the  $\text{Sb}_2\text{Te}_3$  compound lie within  $\delta \sim 5.1\text{--}5.5$  mm/s, which is typical for the spectra of  $^{121}\text{Sb}$  trivalent antimony compounds. It should be concluded that the local structure of the antimony atoms in all of the films studied is close to the local structure of the antimony atoms in the compound  $\text{Sb}_2\text{Te}_3$ . Crystalline antimony telluride has a rhombohedral structure [18]. It contains two types of octahedral positions, differing in the degree of distortion, which are occupied by trivalent antimony atoms. Only divalent tellurium atoms are in the local environment of antimony.

Thus, the MS data confirm the conclusions of the authors [9,15] that the local arrangement of atoms around the Sb atom during the crystallization of the amorphous film  $\text{Ge}_2\text{Sb}_2\text{Te}_5$  remains practically unchanged, i.e., structural changes occur within the local arrangement of Sb atoms, which play the role of the core of the overall structural stability (with the specification that this is true for all GaSbTe alloys).

### 3.4. Tellurium atoms in amorphous and crystalline GeSbTe films

The isomeric shifts of the spectra  $^{125}\text{Te}$  of the films  $a\text{-GeSbTe}$  and  $c\text{-GeSbTe}$  are close to the parameters of the spectra  $^{125}\text{Te}$  of the divalent tellurium  $\text{GeTe}$  and  $\text{Sb}_2\text{Te}_3$  compounds. Therefore, Figs. 5 and 6 show the decomposition of the experimental spectra of  $a\text{-GeSbTe}$  and  $c\text{-GeSbTe}$  films into two singlet spectra with parameters close to those of the  $^{125}\text{Te}$  spectra of  $\text{GeTe}$  ( $\delta = 1.23(4)$  mm/s,  $G = 6.90(8)$  mm/s) and  $\text{Sb}_2\text{Te}_3$  ( $\delta = 1.38(4)$  mm/s,  $G = 6.90(8)$  mm/s), and the amplitudes of the spectra components for the films were varied according to the chemical composition of the films. The satisfactory agreement between the calculated and experimental spectra of  $^{125}\text{Te}$  films allows us to conclude that in crystalline and amorphous films the local structures of tellurium atoms correspond to the structural units of  $\text{GeTe}$  and  $\text{Sb}_2\text{Te}_3$  compounds. The first of these has a NaCl-type lattice with a rhombohedral distortion, and in the immediate vicinity of the divalent six-coordinated tellurium atoms, there are germanium atoms [29]. The second has a structure containing sheets of five atoms thick in the

order  $\text{Te}\text{--Sb}\text{--Te}\text{--Sb}\text{--Te}$ , with the tellurium atoms of the boundary layers forming only three bonds, while the tellurium atoms within the layers form six bonds with the antimony atoms [20].

## Conclusion

The local environment of atoms in amorphous and crystalline films  $(\text{GeTe})_x(\text{Sb}_2\text{Te}_3)$  (where  $x = 0.5, 1, 2, 3$ ) was determined by the MS method on isotopes  $^{119}\text{Sn}$ ,  $^{121}\text{Sb}$  and  $^{125}\text{Te}$ . Impurity tin atoms in the structure of amorphous films isovalently replace the tetravalent germanium atoms, which form a tetrahedral system of chemical bonds (the local coordination number of germanium atoms in amorphous films is four), and in the local environment of germanium atoms are predominantly tellurium atoms. Distortions of the angles between the bonds of germanium (tin) atoms with tellurium atoms in its vicinity lead to a broadening of the spectrum due to unresolved quadrupolar splitting. Fluctuations in the distances from the germanium (tin) atoms to the tellurium atoms while maintaining the tetrahedral system of chemical bonds will lead to a broadening of the spectrum due to a heterogeneous isomer shift.

The MS data on impurity atoms  $^{119}\text{Sn}$  for crystalline films are consistent with the results of X-ray diffraction studies — divalent tin replaces divalent germanium in a rhombohedral distorted NaCl-type lattice. The broadening of the Messbauer spectra of crystal ternary compounds  $(\text{GeTe})_x(\text{Sb}_2\text{Te}_3)$  is associated both with lattice distortion and with the presence of large concentrations of stoichiometric vacancies in the cation sub-lattice of these compounds.

It is concluded that the local structure of both antimony and tellurium atoms in amorphous and crystalline  $(\text{GeTe})_x(\text{Sb}_2\text{Te}_3)$  films is close.

## Conflict of interest

The authors declare that they have no conflict of interest.

## References

- [1] D. Lencer, M. Salinga, M. Wuttig. Adv. Mater., **23**, 2030 (2011). DOI:10.1002/adma.201004255
- [2] C. Qiao, Y.R. Guo, J.J. Wang, H. Shen, S.Y. Wang, Y.X. Zheng, R.J. Zhang, I.Y. Chen, C.Z. Wang, K.M. Ho. J. Alloys and Compounds, **774**, 748 (2019). DOI:10.1063/5.0067157
- [3] B. Zhang, X.P. Wang, Z.J. Shen, X.B. Li, C.S. Wang, Y.J. Chen, J.X. Li, J.X. Zhang, Z. Zhang, S.B. Zhang, X.D. Han. Sci. Rep., **6**, 25453 (2016). DOI: 10.1038/srep25453
- [4] Xue-Peng Wang, Xian-Bin Li, Nian-Ke Chen, Qi-Dai Chen, Xiao-Dong Han, Shengbai Zhang, Hong-Bo Sun. Acta Mater., **136**, 242 (2017). DOI:10.1016%2fj.actamat.2017.07.006&partner

- [5] Z. Sun, S. Kyrsta, D. Music, R. Ahuja, J.M. Schneider. *Solid State Commun.*, **143**, 240 (2007). DOI: 10.1016/j.ssc.2007.05.018
- [6] P. Urban. *Cryst. Eng. Comm.*, **15**, 4823 (2013). DOI: 10.1039/C3CE26956F
- [7] A. Lotnyk, U. Ross, S. Bernütz, E. Thelander, B. Rauschenbach. *Sci. Rep.*, **6**, 26724 (2016). DOI: 10.1038/srep26724
- [8] Y. Zheng, Y. Wang, T. Xin, Y. Cheng, R. Huang, P. Liu, M. Luo, Z. Zhang, Z. Song, S. Feng. *Commun. Chem.*, **2**, 1 (2019). DOI: 10.1038/s42004-019-0114-7
- [9] A.V. Kolobov, P. Fons, A.I. Frenkel, A.L. Ankudinov, J. Tominga, T. Uruga. *Nat. Mater.*, **3**, 703 (2004). DOI: 10.1038/nmat1215
- [10] D.A. Baker, M.A. Paesler, G. Lucovsky, S.C. Agarwal, P.C. Taylor. *Phys. Rev. Lett.*, **96**, 255501 (2006). DOI: 10.1103/PhysRevLett.96.255501
- [11] D.A. Baker, M.A. Paesler, G. Lucovsky, S.C. Agarwal, P.C. Taylor. *J. Non-Cryst. Solids*, **352**, 1621 (2006). DOI: 10.1016/j.jnoncrsol.2005.11.079
- [12] P. Jóvári, I. Kaban, J. Steiner, B. Beuneu, A. Schöps, M.A. Webb. *Phys. Rev. B*, **77**, 035202 (2008). DOI: 10.1103/PhysRevB.77.035202
- [13] Z. Sun, J. Zhou, R. Ahuja. *Phys. Rev. Lett.*, **96**, 055507 (2006). DOI: 10.1103/PhysRevLett.96.055507
- [14] M. Jung, H.J. Shin, K. Kim, J.S. Noh, J. Chung. *Appl. Phys. Lett.*, **89**, 043503 (2006). DOI: 10.1063/1.2236216
- [15] J.R. Stellhorn, S. Hosokawa, S. Kohara. *Analytical Sci.*, **36**, 5 (2020). DOI: 10.2116/analsci.19SAR02
- [16] A.V. Marchenko, P.P. Seregin, E.I. Terukov, K.B. Shakhovich. *Semiconductors*, **53**, 711 (2019). DOI: 10.1134/S1063782619050166
- [17] P.P. Seregin, V.P. Sivkov, F.S. Nasredinov, L.N. Vasilev, Yu.V. Krylnikov, Y.P. Kostikov. *Phys. Stat. Sol. (a)*, **39**, 437 (1977).
- [18] G.A. Bordovsky, A.V. Marchenko, F.S. Nasredinov, Ya.A. Petrushin, P.P. Seregin. *FKhS*, **47**, 179 (2021). DOI: 10.31857/S0132665121020037  
[G.A. Bordovskii, A.V. Marchenko, F.S. Nasredinov, Ya.A. Petrushin, P.P. Seregin. *Glass Phys. Chem.*, **47**, 166 (1921). DOI: 10.1134/S1087659621020036]
- [19] A.V. Marchenko, E.I. Terukov, F.S. Nasredinov, Ya.A. Petrushin, P.P. Seregin. *FTP*, **55**, 3 (2021). DOI: 10.21883/TP.2022.11.55175.186-22 [A.V. Marchenko, E.I. Terukov, F.S. Nasredinov, Ya.A. Petrushin. *Semiconductors*, **55**, 1 (1921). DOI: 10.1134/S1063782621010127]
- [20] F. Ledda, C. Muntoni, A. Rucci, S. Serici, G. Alonzo, M. Consiglio, T. Bressani. *Hyperfine Interactions*, **41**, 591, (1988).
- [21] S. Rigamonti, G. Petrini. *Phys. Stat. Sol. (a)*, **41**, 591 (1970).
- [22] G.A. Bordovsky, E.I. Terukov, N.I. Anisimova, A.V. Marchenko, P.P. Seregin. *FTP*, **43**, 1232 (2009). [G.A. Bordovskii, E.I. Terukov, N.I. Anisimova, A.V. Marchenko, P.P. Seregin. *Semiconductors*, **43**, 1193 (2009). DOI: 10.1134/S1063782609090164]
- [23] M. Micoulaut, K. Gunasekera, S. Ravindren, P. Boolchand. *Phys. Rev. B*, **90**, 094207 (2014). DOI: 10.1103/PhysRevB.90.094207
- [24] P. Boolchand, B.B. Triplett, S.S. Hanna. *Mössbauer Effect Methodology* (New England Nuclear Corporation, 1974)
- [25] M.K. Gauer, I. Dezsi, U. Gonser, G. Langouche, H. Rupperberg. *J. Non-Cryst. Solids*, **101**, 31 (1988). DOI: 10.1016/0022-3093(88)90365-1
- [26] M.K. Gauer, I. Dezsi, U. Gonser, G. Langouche, H. Rupperberg. *J. Non-Cryst. Solids*, **109**, 247 (1989). DOI: 10.1016/0022-3093(88)90365-1
- [27] R. Mantovan, R. Fallica, A. Mokhles Gerami, T.E. Molhol, C. Wiemer, M. Longo, H.P. Gunnlaugsson, K. Johnston, H. Masenda, D. Naidoo, M. Ncube, K. Bharuth-Ram, M. Fanciulli, H.P. Gislason, G. Langouche, S. Glafsson, G. Weyer. *Scientific Rep.*, **7**, 8234 (2017). DOI: 10.1038/s41598-017-08275-5
- [28] R.W. Olesinski, G.J. Abbaschian. *Bulletin of Alloy Phase Diagrams*, **5**, 265 (1984).
- [29] T. Chattopadhyay, J.X. Boucherle, H.G. von Schnering. *J. Phys. C*, **20**, 1431 (1987).
- [30] K. Bobokhuzhaev, A. Marchenko, P. Seregin. *Structural and Anti-Structural Defects in Chalcogenide Semiconductors. Mössbauer Spectroscopy* (LAP Lambert Academic Publishing, 2020)